

# Thermodynamic effects of solid electrolyte interphase formation from solvation and ionic association in water-in-salt electrolytes

Daniel M. Markiewitz,<sup>1,\*</sup> Michael McEldrew,<sup>1</sup> Conor M. E. Phelan,<sup>2</sup>  
Qianlu Zheng,<sup>3</sup> Jasper Singh,<sup>1,2</sup> Robert S. Weatherup,<sup>2,4,5</sup> Rosa M.  
Espinosa-Marzal,<sup>3,6</sup> Martin Z. Bazant,<sup>1,7,†</sup> and Zachary A. H. Goodwin<sup>2,8,‡</sup>

<sup>1</sup>*Department of Chemical Engineering,  
Massachusetts Institute of Technology,  
Cambridge, Massachusetts 02139, United States*

<sup>2</sup>*Department of Materials, University of Oxford,  
Parks Road, Oxford OX1 3PH, United Kingdom*

<sup>3</sup>*Department of Civil and Environmental Engineering,  
The Grainger College of Engineering,  
University of Illinois Urbana-Champaign, Urbana, Illinois 61801, United States*

<sup>4</sup>*Diamond Light Source, Didcot, Oxfordshire OX11 0DE, United Kingdom*

<sup>5</sup>*The Faraday Institution, Quad One, Harwell Science  
and Innovation Campus, Didcot OX11 0RA, UK*

<sup>6</sup>*Department of Materials Science and Engineering,  
The Grainger College of Engineering,  
University of Illinois Urbana-Champaign, Urbana, Illinois 61801, United States*

<sup>7</sup>*Department of Mathematics, Massachusetts Institute of Technology,  
Cambridge, Massachusetts 02139, United States*

<sup>8</sup>*John A. Paulson School of Engineering and Applied Sciences,  
Harvard University, Cambridge, Massachusetts 02138, United States*

(Dated: March 2, 2026)

## Abstract

Water-in-Salt-Electrolytes (WiSEs) are a promising class of next-generation electrolytes. Unlike classical dilute electrolytes or more conventional battery electrolytes, WiSEs are characterised by their super-concentrated salt concentration with only a small amount of water, which gives rise to their expanded electrochemical stability window (ESW). The expansion of the ESW is, in part, due to the formation of an inorganic solid electrolyte interphase (SEI) that passivates the anode; this principle is also important in graphite and Li-metal anodes, and beyond Li-ion technologies. The solvation and ionic associations are key descriptors in understanding the expansion of the ESW. Specifically, as reactions which lead to the SEI (or cathode electrolyte interphase, CEI) must occur at the electrode-electrolyte interface, the distribution of reactants and their various solvation environments are critical. This distribution near the interface is referred to as the electrical double layer (EDL), in the absence of reactions. Here we further develop and analyse a recently proposed thermodynamic theory of hydration and ionic associations in the EDL of WiSEs. We parameterize this theory from bulk molecular dynamics simulations and benchmark it against EDL simulations, finding good qualitative agreement. Using this thermodynamic theory, we rationalise changes in the ESW through: changes in the activity in the bulk electrolyte through the Nernst equation, which directly changes the stability of the electrolytes; and thermodynamic changes to the kinetics of these reactions, from the Butler-Volmer equation and coupled ion electron transfer kinetics, through the concentration of reactant species in the Helmholtz layer. Overall, the presented formalism directly links solvation and ionic aggregation effects to these changes in reactivity, providing key insights into the thermodynamic effects that influence SEI formation in WiSEs. This formalism can be applied to other liquid electrolytes, such as conventional carbonate electrolytes, solvent-in-salt, or Na-ion electrolytes, to understand how solvation and ionic associations expand the ESW and form the SEI.

---

\* dmm385@mit.edu

† bazant@mit.edu

‡ zac.goodwin@materials.ox.ac.uk

## I. INTRODUCTION

Lithium-ion batteries (LIBs) have transformed many technologies in the past decades, such as portable electronic devices, transportation and grid-level storage of renewable energy [1–9]. A prototypical chemistry in a LIB is a mixture of carbonate based solvents, such as ethylene (EC) carbonate and ethyl methyl carbonate (EMC), with  $\text{LiPF}_6$ , at concentrations of  $\sim 1\text{M}$ , often with additives to achieve the desired performance [1, 3, 10]. While LIBs are still becoming cheaper every year, the development of novel chemistries remains highly active, to achieve improvements in safety, capacity and lifetime, amongst other goals [1–9]. These advancements are largely being pursued through changing the electrodes of LIBs - which comprise much of the space, weight, and cost of LIB [11] - to Li-metal anodes [12–14], higher energy density cathodes [15], and beyond Li-ion chemistry [16–18], for example. However, the electrolyte that transports the  $\text{Li}^+$  ions (or other active ions) between the electrodes is still of fundamental importance [19–31], as all components must work efficiently together. For instance, the formation of the interphases between the electrodes and the electrolytes, where on the anode side there is the solid electrolyte interphase (SEI) and the cathode there is the cathode electrolyte interphase (CEI). These interphases form from the degradation of the electrolyte and electrode, but its formation greatly improves Coulombic efficiency by suppressing continuous electrolyte decomposition, which is key for long-term health of the battery [1–9].

Understanding SEI and CEI formation is challenging since it occurs at a solid-liquid interface, where electron transfer processes and reactions occur, over length and time scales that exceed what is feasible with conventional atomistic modeling approaches [1–9]. Machine learning interatomic potentials (MLIPs) are promising to revolutionize this area [32, 33]. Unfortunately these methods can be difficult to train for such electrolytes, often don't have long-range electrostatics and including information about reaction barriers can also be challenging [34–37]. Therefore, there is still motivation for the development of simple, analytical approaches that aid our understanding of interphase formation.

It is well established in the battery community that the coordination environments of  $\text{Li}^+$  (or active cations) correlate with Coulombic efficiency, transport properties, and interphase formation, amongst other properties [9, 38–55]. In terms of interphase formation, the reactions present are often understood in terms of changes to frontier orbitals (HOMO and

LUMO levels), and how these depend on the coordination structure of the electrolyte [48, 54–58]. However, computing these properties for an electrolyte is costly, and even more so if these environments near the interface are studied [58]. Recently there has been progress in understanding the changes in stability/reactivity from thermodynamic effects, such as through changes in activity. One such example is the liquid Madelung potential, as proposed by Takenaka *et al.* [59], which links  $\text{Li}^+$  activity to the electrostatic potential it feels in the electrolyte. Another example is the thermoreversible ionic aggregation and solvation theory of McEldrew *et al.* [60], which directly links coordination environments to activity [61], amongst other properties [62–64]. These changes in activity directly translate to shifts in redox potentials through the Nernst equation, which thermodynamically change the stability of the electrolyte [61] and are linked to changes in frontier orbitals [65].

Another aspect that is important to understanding interphase formation is the electrical double layer (EDL), i.e. what accumulates in the electrolyte at a charged interface [66–68]. This is because what reacts to form the SEI/CEI has to be present at the interface for the electron transfer reactions to occur, with classical rate expressions for these being proportional to the concentration of the reactants [69]. Since simulating the EDL of electrolytes is costly and challenging, it motivates the development of simple approaches. Many theories for predicting the EDL structure exist, such as simple local density approximations [66–68] or more complicated such as the mean-spherical approximation [70]. In LIBs specific interactions between ions and solvent are important, and having an approach which can capture these interactions is essential [64]. As far as we are aware, the only theory which can link consistently predict coordination environments in the EDL is the work of Goodwin and Markiewitz *et al.* [64, 71–74], which is an extension of the earlier work from McEldrew *et al.* [60–63]. This approach has only been investigated for several electrolytes, such as ionic liquids (ILs) [62], salt-in-ILs [63, 72], water-in-salt electrolytes (WiSEs) [61, 73] and conventional battery electrolytes [74, 75].

WiSEs are a promising class of electrolytes for applications in batteries [21, 76–81], owing to their improved safety from the water based solvent, but where the high 21m concentration of LiTFSI (or other IL anions) extends the electrochemical stability window (ESW) up to 4 V, in contrast to dilute water-based electrolytes [40, 61, 80, 82–84]. Moreover, the ionic associations and hydration of  $\text{Li}^+$  are known to be important in 21m, as a percolating ion networks have been found with interpenetrating water domains which still allow for facile

transport of  $\text{Li}^+$  ions [41, 61, 85–92]. McEldrew and Markiewitz *et al.* [61, 73, 83] have previously investigated the bulk stability and EDL properties at lower concentrations, gaining insight into the role of ionic associations and hydration on the activity and EDL of WiSEs. However the 21 m WiSE EDL has not been investigated before with this approach [73], which is the most promising case for battery technologies.

In this paper, we investigate the bulk and EDL of 21 m LiTFSI WiSE from molecular dynamics simulations (MD) and theory to gain insights into the thermodynamic effects that influence electrolyte stability and interphase formation. Initially, we outline our theory for hydration and ionic associations of LiTFSI WiSEs, and we report how we’ve extended our analysis to investigate the EDL properties at the 21 m concentration. This theory is validated against atomistic MD simulations of the EDL of 21 m LiTFSI, where we find good qualitative agreement. Having validated the theory further, we discuss the consequences of its thermodynamic predictions in terms of solid electrolyte interphase formation, starting from the bulk stability changes with concentration, and then moving into thermodynamic effects for the kinetics of these reactions, under certain conditions. After which, we further describe how this formalism can be generalized to other electrolytes of interest for Li-metal anodes (or otherwise), and discuss how the role of the electrode needs to be further incorporated into the model.

## II. THEORY

Here, we present an overview of the EDL theory of WiSEs with thermoreversible associations, since it is important to understand the details of the predicted changes in thermodynamic stability of the electrolyte, and its implications for SEI formation. In Refs. 60–65, 71–75, the theory is outlined in more detail for WiSEs, and other electrolytes, in the bulk and at electrified interfaces, if further information is required.

The WiSE system studied here comprises of cations (+), anions (–), and water (0). These species are assumed to exist in an incompressible lattice-gas [61]. We define the volume of a lattice site to be that of a water molecule,  $v_0$ . The volumes of the other species are expressed relative to  $v_0$  through the number of lattice sites they occupy,  $\xi_j = v_j/v_0$ .

To treat correlations beyond mean-field, we consider the formation of associations between cations and anions, and between cations and water [60, 61]. We do not consider associations

between anions and water, and between water molecules, as these have been shown to be smaller effects. Cations form a maximum of  $f_+$  associations, anions form a maximum of  $f_-$  associations, and water forms a maximum of 1 association; referred to as the functionality of a species [60, 61]. Since  $f_{\pm} > 1$  for WiSEs, a polydisperse set of Cayley tree clusters form, which can be uniquely classified by the rank  $lms$ , i.e., the number of cations  $l$ , anions  $m$ , and water  $s$  in the cluster [60, 61]. The Cayley tree assumption is necessary to keep this theory analytically tractable and physically intuitive. This assumption has been shown to work well for WiSE, and a variety of other concentrated electrolytes [61–63, 65, 75, 93]. When  $f_{\pm} \geq 2$ , which is typical for WiSEs, a percolating ionic network (also referred to as a gel) can form [60].

One of the central variables of our theory is the volume fraction of each species,  $\phi_j$ , where  $j$  is  $+$ ,  $-$ ,  $0$ , or the dimensionless concentrations of species  $c_j = \phi_j/\xi_j$ . A quantity we aim to find from our theory is the dimensionless concentrations of each cluster rank,  $c_{lms}$ . When a gel phase exists we split up the total volume fractions into sol and gel contributions,  $\phi_j = \phi_j^{sol} + \phi_j^{gel}$ , where these volume fractions are determined from Flory's post-gel convention. Finally, the dimensionless concentration of each species can be written as  $c_j = \sum_{lms} i c_{lms} + c_j^{gel}$ , where  $i$  is  $l, m, s$  for  $j$  is  $+, -, 0$ , respectively.

Following Ref. 73 the free energy functional ( $\mathcal{F}$ ) is

$$\begin{aligned} \beta\mathcal{F} = & \int_V d\mathbf{r} \left\{ -\beta \frac{\epsilon_0 \epsilon_r}{2} (\nabla\Phi)^2 + \beta \rho_e \Phi - \frac{c_{001}}{v_0} \ln \left( \frac{\sinh(\beta d |\nabla\Phi|)}{\beta d |\nabla\Phi|} \right) \right\} \\ & + \frac{1}{v_0} \int_V d\mathbf{r} \left\{ \sum_{lms} (c_{lms} \ln \phi_{lms} + \beta c_{lms} \Delta_{lms}) + \beta \Delta_+^{gel} c_+^{gel} + \beta \Delta_-^{gel} c_-^{gel} + \beta \Delta_0^{gel} c_0^{gel} \right\} \\ & + \int_V d\mathbf{r} \left\{ \Lambda \left( 1 - \sum_{lms} (\xi_+ l + \xi_- m + s) c_{lms} - \xi_+ c_+^{gel} - \xi_- c_-^{gel} - c_0^{gel} \right) \right\}. \end{aligned} \quad (1)$$

Here  $\beta = 1/k_B T$  is inverse thermal energy. The first three terms (first line of the functional) represent the electrostatic contribution to the free energy, where  $\epsilon_0$  and  $\epsilon_r$  are, respectively, the vacuum and relative permittivity,  $\Phi(\mathbf{r})$  is the electrostatic potential,  $\rho_e(\mathbf{r}) = e(c_+ - c_-)/v_0$  is the charge density with  $e$  being elementary charge, and  $c_{001}$  and  $d$  are, respectively, the dimensionless concentration of free water and its dipole moment, which is assumed to be behaving as a fluctuating Langevin dipole [73, 83]. The fourth term (first on the second line) is the ideal entropy from the clusters. The fifth term (second on the second line) is the free energy of forming clusters, where  $\Delta_{lms}$  is the free energy of forming a cluster of rank  $lms$ .

The sixth, seventh, and eighth terms (remaining terms on second line) represent the free energy of species associating with the gel,  $\Delta_j^{gel}$ . The final term (third line) is the Lagrange multiplier,  $\Lambda(\mathbf{r})$ , which is used to enforce the incompressibility in the EDL [72, 73].

We consider  $\Delta_{lms}$  to have of three contributions

$$\Delta_{lms} = \Delta_{lms}^{comb} + \Delta_{lms}^{bind} + \Delta_{lms}^{conf}, \quad (2)$$

where  $\Delta_{lms}^{comb}$  is the combinatorial entropy,  $\Delta_{lms}^{bind}$  is the binding energy, and  $\Delta_{lms}^{conf}$  is the configurational entropy.

The combinatorial entropy for the WiSEs Cayley tree clusters [61, 73] is given by

$$\Delta_{lms}^{comb} = -k_B T \ln\{f_+^l f_-^m W_{lms}\}, \quad (3)$$

where

$$W_{lms} = \frac{(f_+ l - l)!(f_- m - m)!}{l!m!s!(f_+ l - l - m - s + 1)!(f_- m - m - l + 1)!}. \quad (4)$$

The binding energy for an  $lms$  cluster with  $l > 0$  is

$$\Delta_{lms}^{bind} = (l + m - 1)\Delta u_{+-} + s\Delta u_{+0}, \quad (5)$$

where  $\Delta u_{+i}$  is the energy of an association between a cation and anion or water [61, 73]. When  $l = 0$ , the binding energy is zero.

Lastly, the configurational entropy is assumed to take the form

$$\Delta_{lms}^{conf} = -\ln\left(\frac{\xi_+ l + \xi_- m + s}{\xi_+^l \xi_-^m}\right) - (l + m - 1)(T\Delta s_{+-} - 1) - s(T\Delta s_{+0} - 1), \quad (6)$$

where  $\Delta s_{+i}$  is the entropy of an association [61, 65].

We can calculate the electrochemical potential of the clusters through taking the derivative of the free energy with respect to  $c_{lms}$

$$\begin{aligned} \beta \bar{\mu}_{lms} = & (l - m)\beta e\Phi - \ln\left(\frac{\sinh(\beta d|\nabla\Phi|)}{\beta d|\nabla\Phi|}\right) \delta_{l,0}\delta_{m,0}\delta_{s,1} + 1 + \ln(\bar{\phi}_{lms}) + \beta\Delta_{lms} \\ & - (\xi_+ l + \xi_- m + s)\Lambda + (\xi_+ l + \xi_- m + s)\beta\bar{g}' \end{aligned} \quad (7)$$

where  $\bar{g}' = \bar{c}_+^{gel} \partial \bar{\Delta}_+^{gel} + \bar{c}_-^{gel} \partial \bar{\Delta}_-^{gel} + \bar{c}_0^{gel} \partial \bar{\Delta}_0^{gel}$ , with the partial derivative being with respect to  $\bar{\phi}_{lms}$ . An overbar indicates that the variable is the EDL version and  $\Phi$  is non-zero, and the absence of it indicates bulk electrolyte, i.e., with zero  $\Phi$ .

In the bulk, chemical equilibrium can be established between free species and aggregates

$$l\mu_{100} + m\mu_{010} + s\mu_{001} = \mu_{lms}, \quad (8)$$

which can be used to find the cluster distribution

$$c_{lms} = \frac{W_{lms}}{\lambda_{+-}} (\psi_{100}\lambda_{+-})^l (\psi_{010}\lambda_{+-})^m (\phi_{001}\lambda_{+0})^s, \quad (9)$$

where  $\psi_{100} = f_+\phi_{100}/\xi_+$  and  $\psi_{010} = f_-\phi_{010}/\xi_-$  are dimensionless concentrations of free lattice sites, and  $\lambda_{+-}$  is the cation-anion association constant and  $\lambda_{+0}$  is the cation-water association constant, given by  $\lambda_{+i} = \exp\{-\beta\Delta f_{+i}\}$ , where  $\Delta f_{+i} = \Delta u_{+i} - T\Delta s_{+i}$  is the free energy of the association.

In order to compute the cluster distribution, we need to know the volume fractions of the *free* species. These, however, are not *a priori* known, and in fact, we wanted to find them from the theory instead of having them as an input. To overcome this obstacle, we introduce association probabilities,  $p_{ij}$ , of  $i$  binding to  $j$  [60, 61]. In an independent association approximation, we can determine the bare species volume fractions as,  $\phi_{100} = \phi_+(1 - p_{+-} - p_{+0})^{f_+}$ ,  $\phi_{010} = \phi_-(1 - p_{-+})^{f_-}$ , and  $\phi_{001} = \phi_0(1 - p_{0+})$ .

While we seem to have simply moved the issue, as we now need to determine the association probabilities which are also not *a priori* known, we can introduce the conservation of associations and the mass action laws of the open and occupied association sites [60, 61] to determine these unknowns. The conservation of cation-anion associations is

$$\psi_+p_{+-} = \psi_-p_{-+} = \zeta \quad (10)$$

where  $\psi_+ = f_+\phi_+/\xi_+$  and  $\psi_- = f_-\phi_-/\xi_-$  are, respectively, the number of cation and anion association sites per lattice site, and  $\zeta$  represents the number of cation-anion associations per lattice site [60, 61]. Similarly, the conservation of cation-water association is,

$$\psi_+p_{+0} = \phi_0p_{0+} = \Gamma \quad (11)$$

where  $\Gamma$  represents the number of cation-water associations per lattice site [60, 61]. The mass action law of cation-anion associations is

$$\lambda_{+-}\zeta = \frac{p_{+-}p_{-+}}{(1 - p_{+-} - p_{+0})(1 - p_{-+})}. \quad (12)$$

For cation-water associations it is

$$\lambda_{+0}\Gamma = \frac{p_{+0}p_{0+}}{(1-p_{+-}-p_{+0})(1-p_{0+})}. \quad (13)$$

Therefore to determine the association probabilities, all we need to know is the association constants, which is another central variable of our theory.

Since the solvation shell of  $\text{Li}^+$  is often full or close to being full, i.e. the number of coordinating species is approximately  $f_+$ . The mass action laws become challenging to solve because  $p_{+-} + p_{+0} \approx 1$  is near a singularity [61]. To overcome the singularity and facilitate a simplified solution, we can introduce the so-called “sticky-cation” approximation, where we assume  $p_{+-} + p_{+0} = 1$  [61]. The created singularities in the law of mass action laws, Eq. (12) & Eq. (13), can be regularized by taking the ratio of these equations,

$$\lambda = \frac{\lambda_{+-}}{\lambda_{+0}} = \frac{p_{-+}(1-p_{0+})}{p_{0+}(1-p_{-+})}, \quad (14)$$

where  $\lambda$  is the cation association constant ratio. Moreover, as the sticky-cation approximation requires  $s = f_+l - l - m + 1$ , the sticky-cation cluster distribution simplifies to

$$c_{lm} = \frac{\phi_0\alpha_0 W_{lm}}{\lambda} \left( \lambda \frac{\psi_+\alpha_{+-}}{\phi_0\alpha_0} \right)^l \left( \lambda \frac{\psi_-\alpha_-}{\phi_0\alpha_0} \right)^m \quad (15)$$

where

$$W_{lm} = \frac{(f_+l - l)!(f_-m - m)!}{l!m!(f_+l - l - m + 1)!(f_-m - l - m + 1)!}. \quad (16)$$

Here,  $\alpha_0 = 1 - p_{0+}$ ,  $\alpha_{+-} = (1 - p_{+-})^{f_+}$  and  $\alpha_- = (1 - p_{-+})^{f_-}$  are the fraction of free water molecules, fully hydrated cations, and free anions, respectively.

Similarly, establishing the equilibrium between the free species and the clusters *within* the EDL [64]

$$l\bar{\mu}_{100} + m\bar{\mu}_{010} + s\bar{\mu}_{001} = \bar{\mu}_{lms}, \quad (17)$$

we obtain an analogous solution for the EDL cluster distribution [64, 73]

$$\bar{c}_{lms} = \frac{W_{lms}}{\lambda_{+-}} (\bar{\psi}_{100}\lambda_{+-})^l (\bar{\psi}_{010}\lambda_{+-})^m (\bar{\phi}_{001}\bar{\lambda}_{+0})^s, \quad (18)$$

where

$$\bar{\lambda}_{+0} = \lambda_{+0} \frac{\beta d |\nabla \Phi|}{\sinh(\beta d |\nabla \Phi|)} \quad (19)$$

as shown above, the cation-water association constant explicitly depends on the electric field. Since the energy of free water changes in the field, but bound water is assumed not to respond to the field [73]. Analogously, we can enforce the sticky-cation approximation in the EDL with  $\bar{p}_{+-} + \bar{p}_{+0} = 1$ , where an equivalent set of conservation of associations and mass action law applies, and we find an analogous sticky-cation cluster distribution,  $\bar{c}_{lm}$ , where  $\bar{\lambda}$  explicitly depends on electric field because of  $\bar{\lambda}_{+0}$ .

Finally to establish an equilibrium between the bulk and the EDL, we set the electrochemical potentials of the free species equal to each other, e.g.,  $\bar{\mu}_{010} = \mu_{010}$  [64]. Following the work of Markiewitz and Goodwin *et al.* [64, 71–74], these can be expressed as so-called Boltzmann closure relations to consistently establish all chemical equilibria. For the anions, we have

$$\bar{\phi}_{010} = \phi_{010} \exp(\beta e \alpha \Phi + \xi_- \Lambda), \quad (20)$$

and for the free water

$$\bar{\phi}_{001} = \phi_{001} \frac{\sinh(\beta d |\nabla \Phi|)}{\beta d |\nabla \Phi|} \exp(\Lambda). \quad (21)$$

Since we will use the sticky-cation approximation, we consider the equilibrium between the fully hydrated cation in the bulk and the EDL

$$\bar{\phi}_{10f_+} = \phi_{10f_+} \exp(-\alpha \beta e \Phi + (\xi_+ + f_+) \Lambda) \quad (22)$$

where  $\phi_{10f_+} = (1 + f_+/\xi_+) \phi_+ (1 - p_{+-})^{f_+}$ . There is, however, freedom in how we choose this closure relationship. For example, we could establish the equilibrium between free cations

$$\bar{\phi}_{100} = \phi_{100} \exp(-\alpha \beta e \Phi + \xi_+ \Lambda). \quad (23)$$

While in the sticky-cation approximation, this is seemingly contradictory, since there are no free cations in the bulk or the EDL, we can regularize this problem to establish a new closure relation

$$\frac{\bar{\phi}_+}{\phi_+} = \left( \frac{\psi_- \bar{p}_{+-} [1 - p_{-+}]}{\psi_- p_{+-} [1 - \bar{p}_{-+}]} \right)^{f_+} \exp(-\alpha \beta e \Phi + \xi_+ \Lambda). \quad (24)$$

Moreover in these closure relations, we introduce the potential rescaling parameter  $\alpha$ , introduced in Ref. 68, to further include correlations beyond the mean-field included so far. Note that formally these closure relationships only hold in the pre-gel regime, since they are obtained from equating the pre-gel chemical potentials [64, 73]. In Ref. 64 it was

shown the gel-terms are small, and that we can extrapolate into the gel regime for ILs [71] and SiILs [72, 93]. However, this extrapolation into the gel in WiSEs regime without modification has not been tested [73], and we test this assumption here.

To predict the EDL properties of WiSEs, we derive our modified Poisson-Boltzmann equation by taking the functional derivative of the free energy with respect to the electrostatic potential

$$\nabla \cdot (\epsilon \nabla \Phi) = -\rho_e = -\frac{e}{v_0}(\bar{c}_+ - \bar{c}_-), \quad (25)$$

where

$$\epsilon = \epsilon_0 \epsilon_r + d \frac{\bar{c}_{001}}{v_0} \frac{L(\beta d |\nabla \Phi|)}{|\nabla \Phi|}. \quad (26)$$

Here  $L(x) = \coth(x) - 1/x$  is the Langevin function. The procedure implemented to solve our system of equations coupled to the modified Poisson-Boltzmann equation is discussed in Ref. 73. Remember, even though the gel terms are neglected in the Boltzmann closure relations, the effect of screening from the gel is still introduced through the charge density in the modified Poisson-Boltzmann equation [64]. Some quantities will be plotted in real space relative to the Debye length,  $\lambda_D$ , or the inverse Debye length,  $\lambda_D^{-1} = \kappa = \sqrt{e^2 \beta (c_+ + c_-) / v_0 \epsilon_0 \epsilon_r}$ .

### III. METHODS

Here we further analyze the constant charge EDL molecular dynamics (MD) simulations from Refs. 83 of 21 m LiTFSI WiSE. Therefore, we refer the reader to Ref. 83 for all the details of those simulations. To compute associations in the MD simulations, we used a real-space cut-off of 2.7 Å between Li<sup>+</sup> and O's in TFSI<sup>-</sup> and H<sub>2</sub>O [73, 83]. For TFSI<sup>-</sup>, we count the associations based on unique anions, so bidentate associations only count as a single association in this model. To calculate the aggregates, we construct an association adjacency matrix. In the EDL, we refer to reader to Ref. 73 for a detailed discussion of how associations are distributed in real-space.

In this work for the volume fractions, we use the same values found in Ref. 61,  $\xi_+ = 0.4$  &  $\xi_- = 10.8$ . Moreover, we pick  $f_+ = 4$  and  $f_- = 3$  [61]. Using these functionalities and the coordination numbers, we can compute the association probabilities through

$$p_{ij} = \left\langle \frac{\# \text{ of associations of type } ij}{f_i \cdot \# \text{ of molecules of type } i} \right\rangle \quad (27)$$

and use the mass action laws to determine the association constants. From the association probabilities, we can compute the association constant using the mass action laws, which then determines all the parameters for our theory. From our analysis of the 21 m water-in-LiTFSI, we found  $\lambda = 0.2527$  and  $v_0 = 21.744 \text{ \AA}^3$ . In addition, we used the following parameters  $\epsilon_r = 10.1$ , and  $P = 4.995$  Debye [83].

## IV. RESULTS

In this section, we validate our proposed EDL theory for 21m LiTFSI WiSE [61, 73] at negative and positive electrodes against atomistic MD simulations [83], which has not been achieved before. Notably, this is because 21m is in the gel regime [61, 73], and the system of equations becomes challenging to solve. Previously, in Ref. 73 the polynomial formulation was investigated. This worked well for the 12 m and 15 m LiTFSI, which is why we used this method. However, it was challenging to solve this system of equations for 21m LiTFSI, which is why this comparison was not shown.

From further testing different approaches for the 21m LiTFSI, we found that overall the Boltzmann closure relations are slightly more numerically well behaved at higher concentrations. As such, we investigated alternative forms of the closure relationship, such as the new one outlined in the Theory Section. However, we found that the hydrated cation Boltzmann closure was more robust than other approaches, as in Eq. (24). Therefore, we stick to this formulation here. Note that these Boltzmann closure relations are formally derived in the pre-gel regime, and additional terms from the gel could be included, but it has previously been found these have a small effect [64]. To further help with numerical solutions and comparisons to experiments, we introduced a consistent charge rescaling parameter [68], which makes the agreement more qualitative than in Ref. 73 for the 12 m and 15 m LiTFSI WiSEs. We used the largest value of  $\alpha = 0.3$  [68] that would allow us to solve the system of equations. Here we use this value for all calculations.

### A. Negative EDL

In Fig. 1, we display our comparison between theory and simulation for the anode of 21m WiSE, where the grey region in the simulations denotes where not all species can be detected

in the MD simulation. This demarcates the onset of where comparison to predictions in the theory should break down and where surface effects can become important (such as blocking of association sites and interactions with the electrode) [73]. Hereon out, we refer to this as the Helmholtz region [74].

First we compare the volume fractions of each species in the EDL,  $\bar{\phi}_i$ , as seen in Figs. 1(a)&(e) for the simulation and theory, respectively. In the simulation, we find oscillations of  $\bar{\phi}_-$  in the diffuse part of the EDL, with a strong decay towards the Helmholtz region, with the anions being completely depleted in this region. On the other hand, we find  $\bar{\phi}_+$  and  $\bar{\phi}_0$  have small oscillations in the diffuse EDL, but they accumulate strongly before the Helmholtz region. Moreover, we find two distinct layers of  $\text{Li}^+$ , one being right at the interface of the electrode in the Helmholtz region, and the other at the boundary of the Helmholtz region with the diffuse EDL, with a substantial water layer between them. The theory predictions are able to qualitatively capture these changes before the Helmholtz region, i.e. the diffuse EDL, but the theory cannot capture the oscillations and layering which occur, since it is a local density approximation. Specifically, the theory predicts a monotonic decay of anions and a monotonic increase of cations and water.

Next we compare the volume fractions of some chosen clusters,  $\bar{\phi}_{lms}$ , see Figs. 1(b)&(f), which allows us to understand the changes in species volume fractions in more detail. In the MD simulations, the volume fraction of free anions,  $\bar{\phi}_{010}$ , remains small throughout the EDL and bulk region, indicating most anions exist in aggregates. Similarly, there's a small volume fraction of hydrated cations and water in the bulk and diffuse EDL, but there's a notable increase in them towards the interface. We find that the two layers of  $\text{Li}^+$  previously described are largely composed of hydrated cations, while the water layer between them is mostly free water. We also quantify the volume fraction of remaining aggregates and gel phase, calculated from  $\bar{\phi}_{Agg} = 1 - \sum_x \bar{\phi}_{10x} - \bar{\phi}_{010} - \bar{\phi}_{001}$ . In the bulk and diffuse EDL, the aggregates/gel are in majority, and only strongly dissipate when in the Helmholtz region, indicating that the aggregates/gel must be contributing substantially to the screening of the electrode. Again, the theory qualitatively captures these changes, in a smooth way, up to the Helmholtz region in the MD simulations.

Finally we discuss how the association probabilities change within the EDL, which as far as we are aware no other theory is able to predict. In Figs. 1(c)&(g) we show  $\bar{p}_{ij}$  from simulation and theory, respectively. In the diffuse region of the simulations there are oscilla-

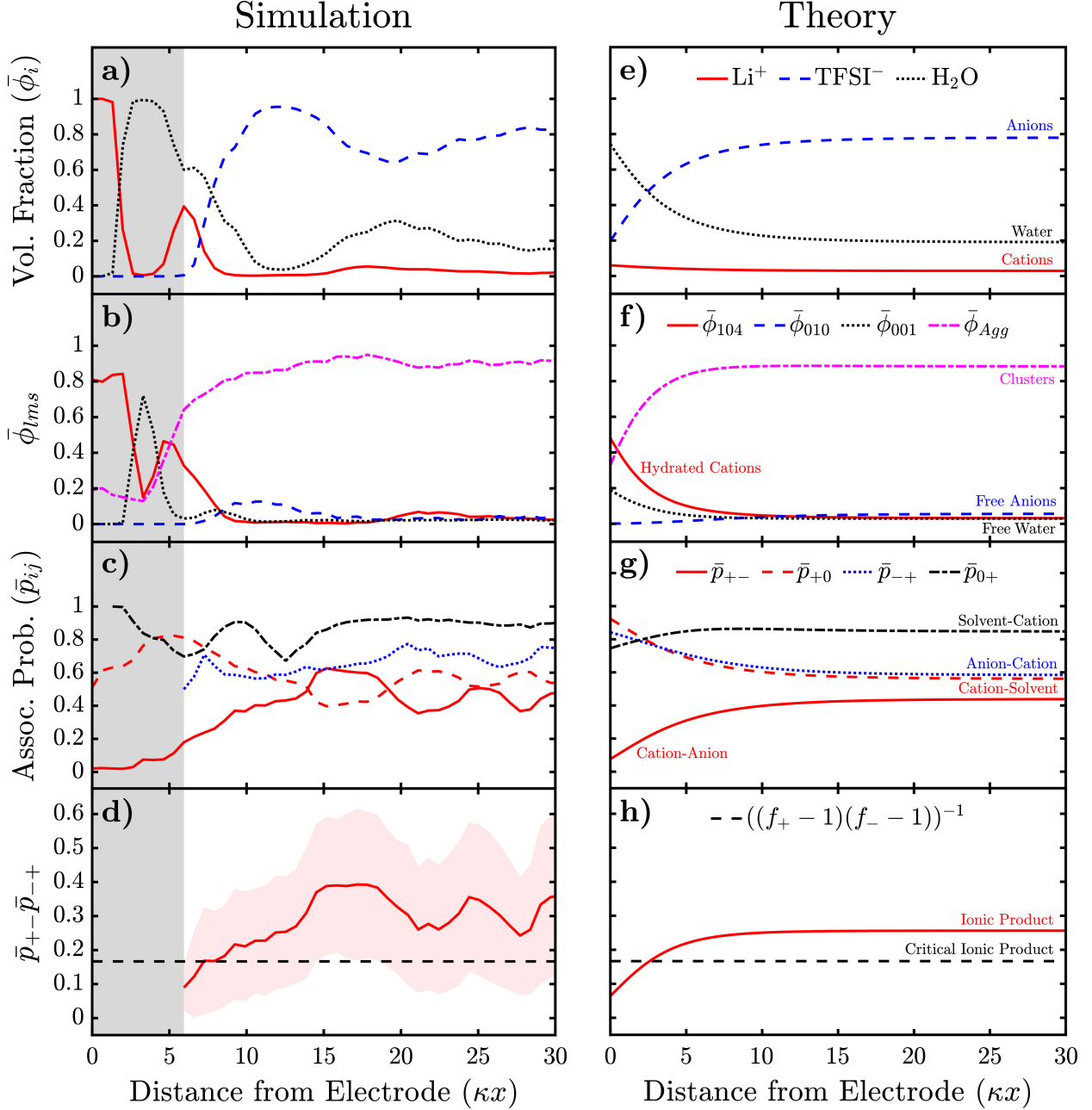


FIG. 1. EDL of 21m WiSEs at negative electrode ( $\sigma = -0.2 \text{ C/m}^2$ ) as a function from the interface, in dimensionless units, where  $\kappa$  is the inverse Debye length, from simulations (a-d) and theory (e-h). In the former, the grey region indicates the minimum distance from the electrode at which a species was never found. a,e) Volume fraction of each species ( $\bar{\phi}_i$ ). b,f) Volume fractions of hydrated cations (Simulation  $\bar{\phi}_{10x}$  & Theory  $\bar{\phi}_{104}$ ), free anions ( $\bar{\phi}_{010}$ ), free water ( $\bar{\phi}_{001}$ ), and aggregates and gel, if present ( $\bar{\phi}_{Agg}$ ). c,g) Association probabilities ( $\bar{p}_{ij}$ ). d,h) Product of the ionic association probabilities,  $\bar{p}_{+-}\bar{p}_{-+}$ , where the dashed line indicates the critical line for gelation and the red shaded region is the standard deviation.

tions in  $\bar{p}_{+0}$  (the probability of cations associating to water), which transition into a steady increase towards the Helmholtz region. In contrast,  $\bar{p}_{0+}$  remains approximately constant, with a slight decrease just before the Helmholtz layer, albeit with some fluctuations. In the theory,  $\bar{p}_{+0}$  steadily increases in the EDL, but  $\bar{p}_{0+}$  steadily decreases. Therefore, our theory has some success in describing these changes in coordination environments.

The cation-anion association probability,  $\bar{p}_{+-}$ , decreases substantially in the EDL from the simulations, while the anion-cation association probability,  $\bar{p}_{-+}$ , remains roughly constant in the simulations. Our theory also predicts  $\bar{p}_{+-}$  to decrease in the EDL, but for  $\bar{p}_{-+}$  to increase to a lesser extent. Our theoretical approach describes well the cation coordination environment, but appears to struggle with the anion coordination environment.

By taking the product of these probabilities,  $\bar{p}_{+-}\bar{p}_{-+}$ , we can determine bond percolation for the Bethe lattice that the aggregates exist on. If  $\bar{p}_{+-}\bar{p}_{-+} > [(f_+ - 1)(f_- - 1)]^{-1}$ , there is a percolating ionic network, i.e. a gel phase. In bulk 21m LiTFSI WiSE, the percolating ionic network is known to exist, with the gel-point being determined to be close to 18m in LiTFSI. In the simulations, as displayed in Fig. 1(d), we see in the bulk and diffuse EDL that a gel phase exists, but close to the Helmholtz region the network is destroyed as this product dips below the critical value, which corresponds well to the reduction in aggregates/gel observed in Fig. 1(b). The theory, shown in Fig. 1(h), is able to capture the changes in the percolating ionic network well, where we predict a gel phase in the bulk and diffuse EDL, but close to the interface the criteria drops below the critical value.

Overall, in Fig. 1 we have demonstrated the overall changes in composition and coordination environments of 21m LiTFSI WiSE EDL at negative electrodes, and found reasonable agreement with the the theory and simulations. As previously discussed, the largest differences between these methods occurs in the Helmholtz region, where not all species are present and surface effects become important. In Ref. 74, it was suggested that an approach to describe the differences in the Helmholtz region was from the interface blocking association sites and interacting with them, manifesting through an apparent reduction in the functionalities,  $f_i$ . If we propose that  $f_+$  changes from 4 to 3 in the Helmholtz region, we might expect to observe a decrease in  $\bar{p}_{+j}$  in the simulations in this region, as a value of 4 was used in Fig. 1, which is what we can see for  $\bar{p}_{+j}$ .

Our approach also allows us to investigate the cluster distribution,  $\bar{c}_{lms}$ , in different regions of the EDL, which we display in Fig. 2 from simulation and theory. Note that we

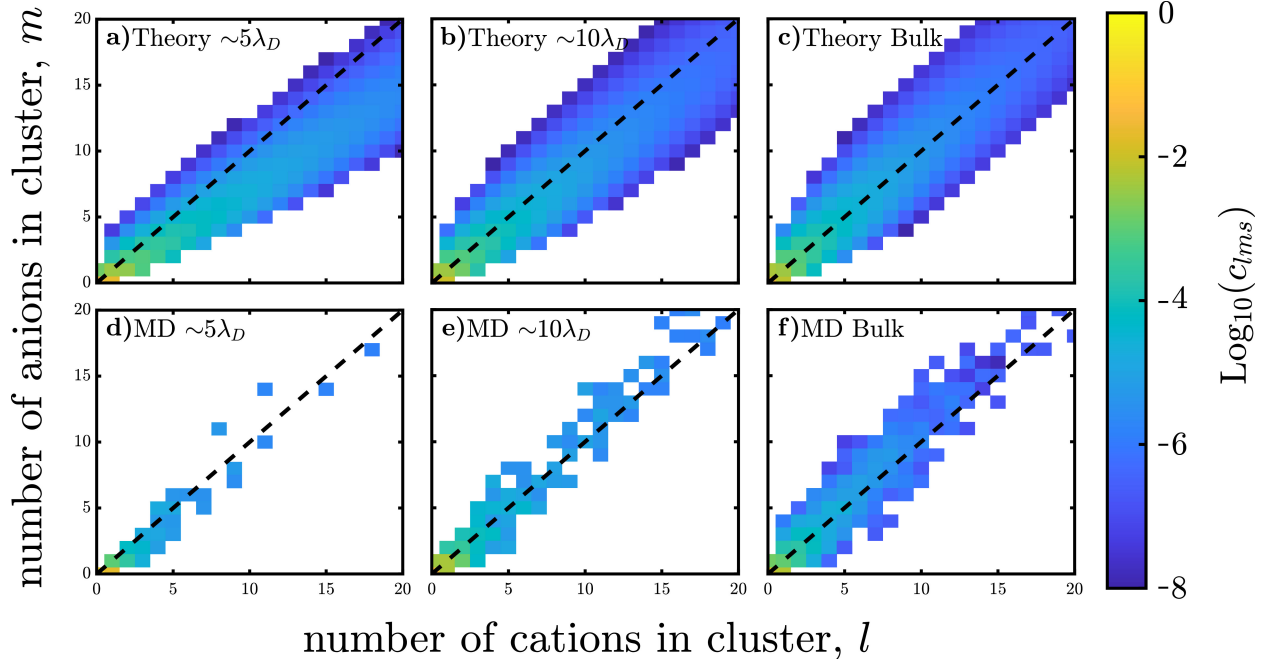


FIG. 2. Cluster distribution of 21m water-in-LiTFSI near the negative electrode ( $\sigma = -0.2 \text{ C/m}^2$ ) at different distances from the interface, from theory (a-c) and simulations (d-f).

use the stick-cation approximation, so we only need to plot  $\bar{c}_{lm}$ . In the bulk, we observe an MD cluster distribution has a slightly negative bias to the aggregates, since  $f_+ > f_-$ , with clusters containing up to 12 cations and 12 anions, as seen in Fig. 2(f). The theory has a similar distribution, see Fig. 2(c), but with a longer tail in the distribution. In the diffuse EDL, at  $\sim 10\lambda_D$  from the interface, we find that the MD cluster distribution has increased concentrations of some larger clusters, consistent with the observation that the gel phase is being dismantled closer to the interface, as displayed in Fig. 2(e). For small clusters ( $l < 5$ ), there is a positive bias of these aggregates, but for larger aggregates there's a negative bias. The theory captures the extended cluster distribution, but predicts a positive bias for all aggregates, shown in Fig. 2(b), indicating a breakdown in our assumed cluster distribution. Finally, just outside the Helmholtz region ( $\sim 5\lambda_D$ ), our simulations [Fig. 2(d)] show a diminished cluster distribution with positive bias, demonstrating the screening ability of these aggregates. The theory, see Fig. 2(a), has a strongly positive bias for the charge of clusters and the cluster distribution has grown relative to the diffuse EDL, which can be attributed to the theory over-predicting the stability of the gel phase  $5\lambda_D$  from the interface.

## B. Positive EDL

In Fig. 3, we compare the EDL predictions from MD simulations and theory for the positive (cathodic) electrodes of 21m LiTFSI WiSE. We display the changes of volume fractions in the EDL in Fig. 3a)&e), from MD and theory, respectively. The simulations predict  $\bar{\phi}_-$  to have a pronounced dip in the diffuse layer, before saturating just outside the Helmholtz region. Right at the interface, however, the anions are completely depleted and there is a substantial water layer. There is also a large accumulation of water in the dip in anion volume fraction in the diffuse EDL. Interestingly, there is a moderate increase in the  $\text{Li}^+$  volume fraction between the dip in  $\bar{\phi}_-$  and the peak in  $\bar{\phi}_0$  (at  $x \approx 9\lambda_D$ ), before it is completely suppressed in the Helmholtz region. The theory predicts more modest changes in the EDL. Cations are slowly, monotonically suppressed towards the interface. In contrast, the anions are initially enriched relative to the bulk, before being depleted closer to the interface, reflecting the MD simulations qualitatively. Similarly, the water is initially depleted in the diffuse layer, before enriching near the interface, also in the non-monotonic dependence observed in the simulations.

Further inspecting the common clusters and free species in the EDL reveals more insights into these changes in volume fraction as shown in Fig. 3b)&f). In the MD, we observe a large increase in free anions,  $\bar{\phi}_{010}$ , around the boundary of the Helmholtz region, which corresponds to the saturation of  $\bar{\phi}_-$  previously described. Similarly, the water layer right at the interface is solely free water. The hydrated cations do not accumulate in the positive EDL. However, we do observe a non-monotonic dependence of the aggregate/gel volume fraction as the electrode interface is approached. In the diffuse EDL, there is a large peak which corresponds well to the increase in  $\text{Li}^+$ , indicating the cations are mainly bound up in aggregates. Moving towards the Helmholtz region, the aggregates/gel is suppressed, but they remain substantial in the middle of the Helmholtz region. The theory agrees reasonably well with these simulations, although the finer, non-monotonic details are missed. We find a strong suppression in hydrated cations and clusters/gel, and an accumulation of free anions and free water.

Next we inspect the changes in association probabilities, as seen in Fig. 3c)&g). From the simulations, we find  $\bar{p}_{+0}$  fluctuates in the bulk and diffuse region before being suppressed near the Helmholtz region. Similarly, we find  $\bar{p}_{0+}$  is strongly suppressed to 0 in the Helmholtz

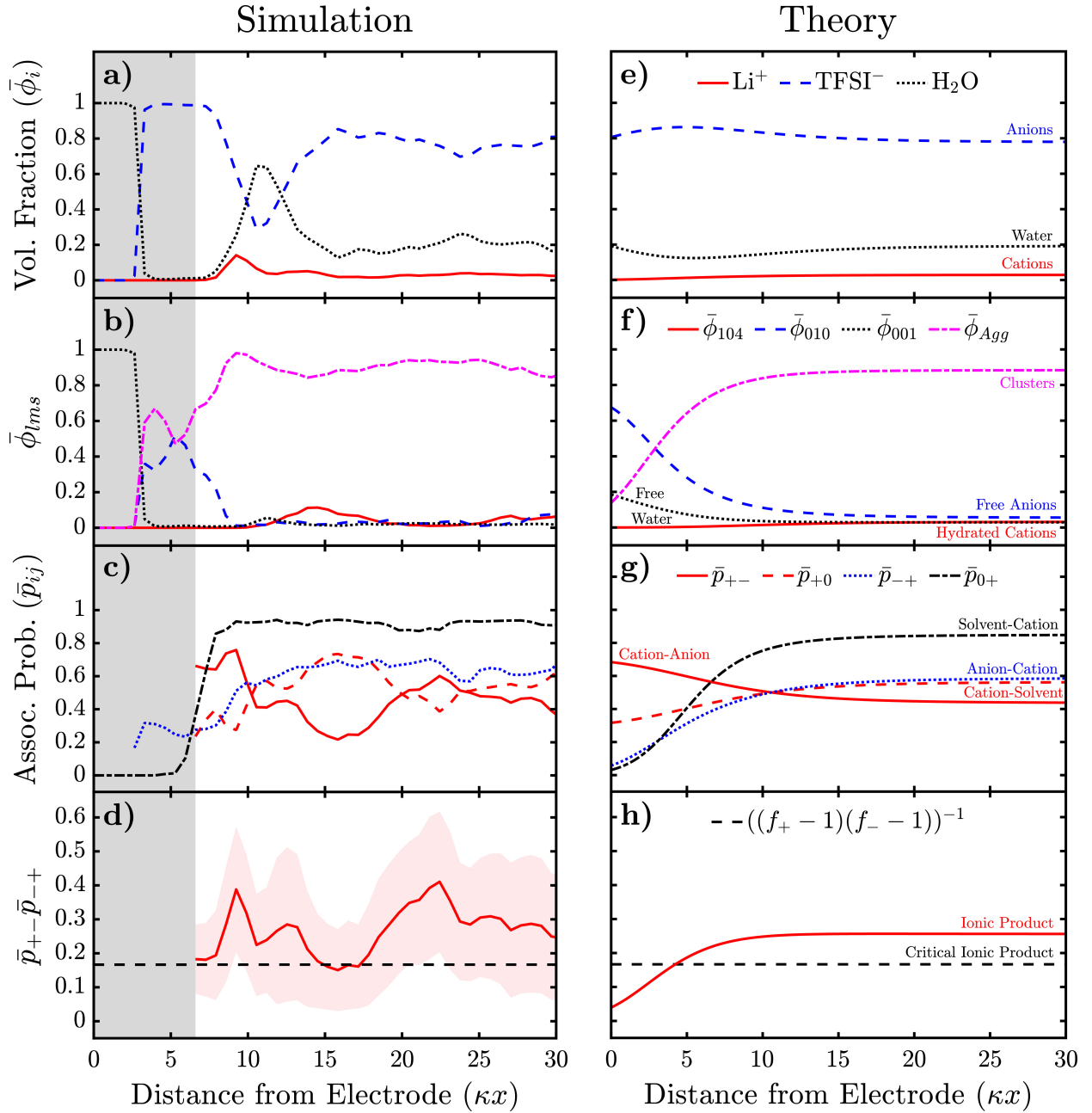


FIG. 3. EDL of 21m WiSEs at positive electrode ( $\sigma = 0.2 \text{ C/m}^2$ ) as a function from the interface, in dimensionless units, where  $\kappa$  is the inverse Debye length, from simulations (a-d) and theory (e-h). In the former, the grey region indicates the minimum distance from the electrode at which a species was never found. a,e) Volume fraction of each species ( $\bar{\phi}_i$ ). b,f) Volume fractions of hydrated cations (Simulation  $\bar{\phi}_{10x}$  & Theory  $\bar{\phi}_{104}$ ), free anions ( $\bar{\phi}_{010}$ ), free water ( $\bar{\phi}_{001}$ ), and aggregates and gel, if present ( $\bar{\phi}_{Agg}$ ). c,g) Association probabilities ( $\bar{p}_{ij}$ ). d,h) Product of the ionic association probabilities,  $\bar{p}_{+-}\bar{p}_{-+}$ , where the dashed line indicates the critical line for gelation, with the shaded region denoting its standard deviation.

region indicating that water prefers to be in the free state. These changes in association probabilities are captured qualitatively by the theory. We find  $\bar{p}_{+-}$  also fluctuates in the bulk/diffuse EDL, before increasing slightly towards the Helmholtz layer. While the anion-cation association probability decreases in the EDL. The theory is able to qualitatively reproduce these changes in the ionic association probabilities.

In Fig. 3d)&h), we investigate where the percolating ionic network survives in the EDL. From the simulations, we find the bulk the gel phase exists, but moving towards the diffuse and Helmholtz regions we find large fluctuations, where it is almost suppressed several times. Within the Helmholtz region no gel phase exists, since we know this is dominated by free water and free cations, with some clusters. We find the theory predicts a monotonically decreasing percolation probability, which just dips below the critical condition at the interface, indicating the gel phase is destroyed there.

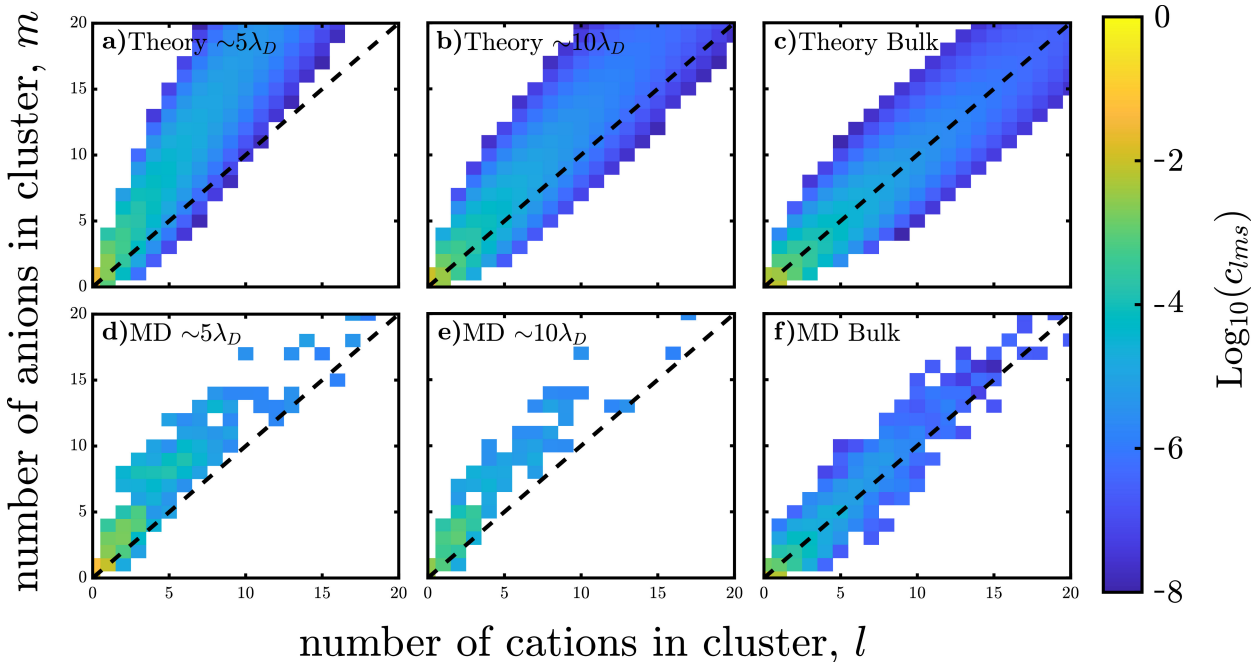


FIG. 4. Cluster distribution of 21m water-in-LiTFSI near the positive electrode ( $\sigma = 0.2 \text{ C/m}^2$ ) at different distances from the interface, from theory (a-c) and simulations (d-f).

In Fig. 4 we further inspect the cluster distribution, from theory and simulation, at various positions in the EDL at positive electrodes. We will not recap the bulk as it was previously described. In the diffuse layer  $\sim 10\lambda_D$  from the interface, the simulations predict a negatively biased cluster distribution. The simulations predict that the concentrations

of the larger clusters increase relative to the the bulk, but some of the larger aggregates are suppressed relative to the bulk. The theory predicts that the cluster distribution has a negative bias and larger clusters exist than the bulk. At  $\sim 5\lambda_D$  similar observations are found from both theory and simulation.

### C. Thermodynamic Stability and Interphase Formation

Having further validated that our theory captures the trends in composition and coordination environments in the EDL of 21m LiTFSI WiSE [73], we turn to using this theory to understand thermodynamic effects that influence stability and interphase formation of these electrolytes [61, 65, 83]. We achieve this through predicting the changes in thermodynamic activity in the bulk and EDL, and changes in concentration within the EDL [61, 73, 83].

We start by deriving expressions for the thermodynamic activity in the bulk with the sticky-cation approximation [61], based on our functional free energy formalism [73]. Generally, the activity of a species,  $a_i$ , can be expressed as

$$\ln a_i = \beta(\mu_i - \mu_i^\theta), \quad (28)$$

where  $\mu_i$  is the chemical potential and  $\mu_i^\theta$  is the reference state chemical potential. Using this definition, we have for the bulk, sticky-cation approximation (neglecting gel terms, as we did for the closure relations) activity of each species

$$\ln(a_+) = \ln\left(\frac{\phi_+}{\phi_+^\theta}\right) + f_+ \ln\left(\frac{p_{+0}}{\psi_0[1-p_{0+}]}\frac{\psi_0^\theta[1-p_{0+}^\theta]}{p_{+0}^\theta}\right), \quad (29)$$

$$\ln(a_-) = \ln\left(\frac{\phi_-}{\phi_-^\theta}\right) + f_- \ln\left(\frac{1-p_{-+}}{1-p_{-+}^\theta}\right), \quad (30)$$

$$\ln(a_0) = \ln\left(\frac{\phi_0[1-p_{0+}]}{\phi_0^\theta[1-p_{0+}^\theta]}\right). \quad (31)$$

Note that with how we establish the chemical equilibrium, the chemical potential of cations (same logic applies to anions and water) in an aggregate is equal to the free cation, and the free cation chemical potential does not depend on the cluster rank, so it is the convenient choice ( $\mu_{lms}^+ = \partial\mu_{lms}/\partial l = \mu_{100} = \mu_+$ ) [60, 61]. In addition, we can also calculate the activity of certain species, such as the hydrated cation

$$\ln(a_{10f_+}) = \ln\left(\frac{\phi_+}{\phi_+^\theta}\right) + f_+ \ln\left(\frac{p_{+0}}{p_{+0}^\theta}\right), \quad (32)$$

which is an important species in WiSEs. Note that in our theory, the activity, which represent the effective concentrations of species, is given by the concentration of free species [60]. This provides a simple and direct link, where all of the non-ideal changes are occurring through the associations.

In Eqs. (29)-(31), we take the reference state to be infinite dilution for the electrolyte. This corresponds to  $\phi_0^\theta = 1$ ,  $p_{+-}^\theta = p_{-+}^\theta = p_{0+}^\theta = 0$ , and  $p_{+0}^\theta = 1$ . We can use this reference state explicitly, but divergences remain. In practice the standard is take a small non-zero concentration of the electrolyte as the reference, which removes these divergences [61].

In Fig. 5, we show the changes in activity as a function of salt concentration from these equations, for water, cations, anions and hydrated cations referenced against the 0.5 m state. Consistent with previous findings [61], we see the water activity decreases with salt concentration, the anion activity initially increases with salt concentration before decreasing again at higher concentrations, and the  $\text{Li}^+$  activity monotonically increases with salt concentration [61]. We find the activity of hydrated cations tracks the activity of the anions.

To understand these changes in activity, all we need to know is how the association probabilities change with salt concentration, which provides the direct link of how activity depends on coordination environments as well as how the volume fractions of species change with salt concentration. In Fig. 6, we show how the association probabilities change with salt concentration. Using this information, we can determine that the anion activity is non-monotonic because of the increase in  $p_{-+}$  dominates over the increase in  $\phi_-$  at large salt concentrations. The cation activity monotonically increases because  $p_{+0}/\psi_0(1 - p_{0+})$  also increases with salt concentration. The activity of water decreases because of a decreasing  $\phi_0$ , but also because of an increasing  $p_{0+}$ .

To understand why the hydrated cation activity follows that of the anion, we expand it in the smallness of  $p_{-+}$  and  $p_{+-}$  at low concentrations to give  $\ln(a_{10f_+}) \approx f_+p_{+-}$ , and  $\ln(a_{010}) \approx f_-p_{-+}$ , which we can see must hold from the conservation of associations. According to hydration theory [94], the difference between the activity of cations and anions can solely be attributed to their different solvation environments. Our observation that the hydrated cation activity is close to the anion activity suggests the hydration theory [94]

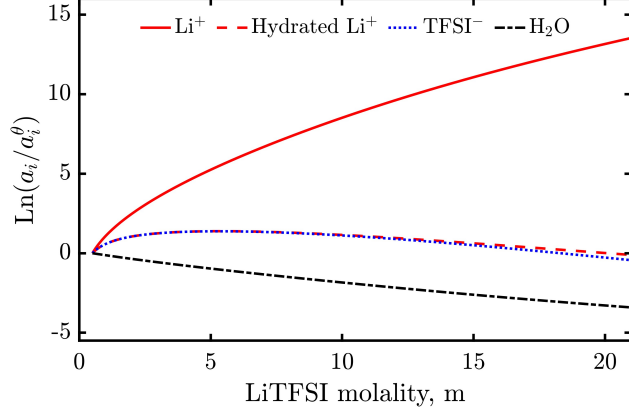


FIG. 5. Activity of ions, water and hydrated cations in the bulk as a function of molality, computed with the sticky cation approximation for LiTFSI.

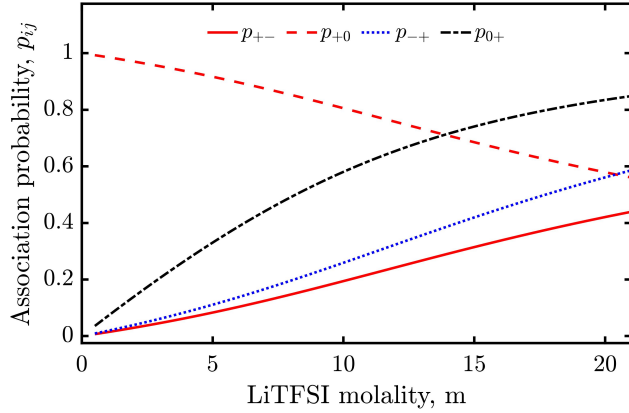
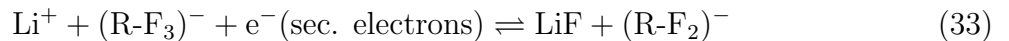


FIG. 6. Association probabilities as a function of salt molality, from 21m down to 0.5m, computed with the sticky-cation approximation for LiTFSI.

could be contained within, or be a limit of, our more general theory.

These changes in activity are a key part of the changes in thermodynamic stability of the electrolyte, and its ability to form a stable interphase. The changes in activity can be directly linked, through the Nernst equation, to changes in redox potentials of reactions which can occur to form the interphases, or parasitic reactions.

Let us consider the SEI reaction from Ref. 95, where the TFSI<sup>-</sup> undergoes reduction and removal of fluoride, which combines with the Li<sup>+</sup>, to form LiF



where R=CF<sub>3</sub>-SO<sub>2</sub>-N-SO<sub>2</sub>-C. The change in the equilibrium reduction potential is given by

the Nernst equation of this reaction

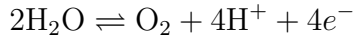
$$E - E^\theta = \frac{k_B T}{e} \ln \left( \frac{a_{\text{Li}^+} a_{(\text{R-F}_3)^-}}{a_{\text{LiF}} a_{(\text{R-F}_2)^-}} \right), \quad (34)$$

Taking the activity of the products are ideal, i.e.,  $a_{\text{LiF}} = 1$  and  $a_{(\text{R-F}_2)^-} = 1$ , we have for the change in equilibrium redox potential

$$E - E^\theta = \frac{k_B T}{e} \ln (a_{\text{Li}^+} a_{(\text{R-F}_3)^-}) = k_B T \ln(a_+ a_-) \quad (35)$$

Therefore, increasing the salt concentration from 0.5 m to 21 m leads to a positive shift of approximately 0.35 eV in electrochemical reactions involving  $\text{Li}^+$ , such as LiF formation in Eq. (33). Similarly, other Li-containing salts formed in the SEI/CEI ( $\text{Li}_x\text{PO}_y\text{F}_z$ ,  $\text{Li}_2\text{O}$ ,  $\text{Li}_2\text{CO}_3$ , and  $\text{LiOH}$ ) [96–98], as well as their associated decomposition reactions[99], will undergo positive shifts in their electrochemical reduction potentials as the concentration increases from 0.5 m to 21 m due to changes in Li activity. Moreover, our theory shows that variations in  $\text{Li}^+$  activity play a significantly larger role in shifting these reduction potentials than changes in TFSI<sup>-</sup> activity, the latter contributing a comparatively small negative shift of approximately -0.1 V over the same concentration range. These shifts lead to significant differences in the chemical composition of the interphases formed at 0.5 m and 21 m.

Next we consider the salt stabilization of water. At positive interfaces, suppression of the oxygen evolution reaction has been reported. Considering the oxidation of water, we have



The Nernst equation for oxygen evolution reaction is

$$E - E^\theta = \frac{k_B T}{4e} \ln \left( \frac{a_{\text{H}_2\text{O}}^2}{a_{\text{H}^+}^4 a_{\text{O}_2}} \right). \quad (36)$$

Assuming the activity of products are ideal,  $a_{\text{H}^+} \approx 1$  (i.e., neglecting the role of pH) and  $a_{\text{O}_2} \approx 1$ , we have

$$E - E^\theta = \frac{k_B T}{2e} \ln (a_{\text{H}_2\text{O}}) = \frac{k_B T}{2e} \ln(a_0). \quad (37)$$

This states changing the salt concentration from 0.5 m to 21 m shifts the oxidation potential of water by -5 mV. Therefore, it becomes more thermodynamically favourable to oxidise

water with increasing salt concentration. This indicates improvements in electrochemical stability for the water arise from kinetic contributions as opposed to thermodynamic contributions at more positive potentials.

In a similar way, consider the reduction of water at negative potentials



The Nernst equation for this reaction is

$$E - E^\theta = \frac{k_B T}{2e} \ln \left( \frac{a_{\text{H}_2\text{O}}^2}{a_{\text{OH}^-}^2 a_{\text{H}_2}} \right). \quad (38)$$

Again, assuming the activity of products are ideal,  $a_{\text{OH}^-} \approx 1$  (i.e., neglecting the role of pH) and  $a_{\text{O}_2} \approx 1$ , we arrive at

$$E - E^\theta = \frac{k_B T}{e} \ln(a_{\text{H}_2\text{O}}) = \frac{k_B T}{e} \ln(a_0). \quad (39)$$

Increasing the salt concentration from 0.5 m to 21 m shifts the reduction potential of water by -10 mV, making water reduction slightly less thermodynamically favorable at higher salt concentrations. This shift contributes, in part, to the apparent expansion of the electrochemical stability window. These results demonstrate that increasing salt concentration appreciably alters SEI composition by promoting the formation of Li salts, while thermodynamically suppressing the reduction of water. While the thermodynamic stability at positive potentials is worsened, kinetic limitations of the OER likely dominate resulting in the improved oxidative stability observed in WiSEs.

Next, we look into the thermodynamic effects which can alter reaction kinetics at the interface [69, 100]. In expressions for the current densities, there is often a linear dependence on the concentration of the species reacting at the interface [100]. The seminal example of which is Butler-Volmer reaction kinetics [100]. Moreover, this intuitively makes sense, since what can react (and form the interphase or evolve gasses) is what is at the interface between the electrode/interphase and the electrolyte, where the electron transfer processes can occur. Therefore, provided we are in a situation where transport limitations are not strong, such that an equilibrium theory can be used, looking at the concentration of key species in the EDL, especially right at the interface, can provide insight into changes in these redox reactions. For the reactions previously discussed, we consider how the concentration of reactants at the interface could influence the rates of these reactions.

For the formation of the inorganic SEI, we can inspect the surface concentrations of  $\text{Li}^+$  and  $\text{TFSI}^-$  [95]. As previously discussed, we found a large concentration of  $\text{Li}^+$  right at the interface of negative electrodes, followed by a layer of water, and at further distances there are significant  $\text{TFSI}^-$  anions. Further inspection showed that much of the  $\text{Li}^+$  and water were there in the form of hydrated  $\text{Li}^+$ , but there was also a significant fraction of clusters. Since these clusters will involve  $\text{Li}^+$ - $\text{TFSI}^-$  at the interface, there should not be any kinetic reasons to limit the formation of  $\text{LiF}$ , and in fact, these clusters should facilitate this reaction. At lower concentrations, as previously studied in Ref. 73, the interface was significantly more populated with hydrated  $\text{Li}^+$  and there was an absence of clusters at the interface. Therefore, with increasing salt concentration, there is an increase in the thermodynamic stability of the electrolyte, but also the initial kinetics of the SEI formation should be more facile, which can also contribute to a longer-term kinetic passivation through the formation of this SEI [95]. On the other hand, for the oxidation of water at  $+0.2 \text{ C/m}^2$  interfaces, we find substantial water right at the interface [95]. While this is a large surface charge, as studied in Refs. 73, 83, at lower surface charges there can be a depletion of water, which would suppress the kinetics of the oxygen evolution reaction.

Not only can we inspect the changes in concentration within the EDL, but we can also derive expressions for the activity within the EDL [101, 102]. Again within the stickysation approximation, neglecting the gel terms and the electrostatic contributions to the electrochemical potential, we arrive at

$$\ln(\bar{a}_-) = \ln\left(\frac{\bar{\phi}_-}{\phi_-^\theta}\right) + f_- \ln\left(\frac{1 - \bar{p}_{-+}}{1 - p_{-+}^\theta}\right) - \xi_- \Lambda, \quad (40)$$

$$\ln(\bar{a}_0) = \ln\left(\frac{\bar{\phi}_0[1 - \bar{p}_{0+}]}{\phi_0^\theta[1 - p_{0+}^\theta]}\right) - \Lambda. \quad (41)$$

$$\ln(\bar{a}_+) = \ln\left(\frac{\bar{\phi}_+}{\phi_+^\theta}\right) + f_+ \ln\left(\frac{\psi_0^\theta \bar{p}_{+0}(1 - p_{0+}^\theta) \sinh(\beta d |\nabla \Phi|)}{\bar{\psi}_0 p_{+0}^\theta (1 - \bar{p}_{0+}) \beta d |\nabla \Phi|}\right) - \xi_+ \Lambda \quad (42)$$

or equivalently,

$$\ln(\bar{a}_+) = \ln\left(\frac{\bar{\phi}_+}{\phi_+^\theta}\right) + f_+ \ln\left(\frac{\psi_-^\theta \bar{p}_{+-}(1 - p_{-+}^\theta)}{\bar{\psi}_- p_{+-}^\theta (1 - \bar{p}_{-+})}\right) - \xi_+ \Lambda, \quad (43)$$

similar to the activity expressions previously stated.

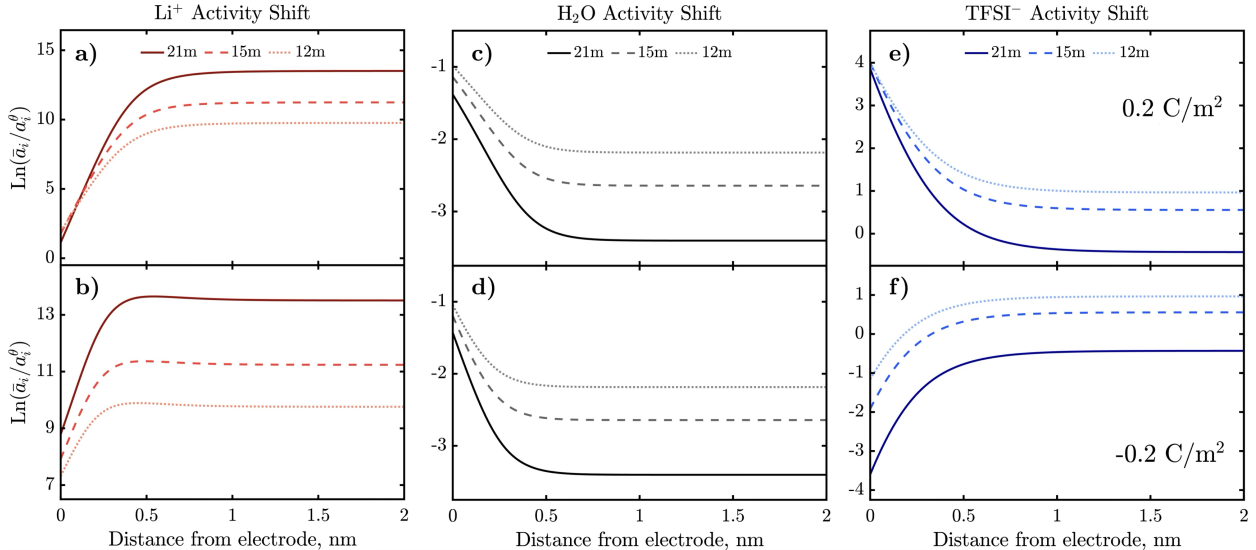


FIG. 7. Activity of species within the EDL for as a function of distance from the electrode, at various concentrations, at the indicated surface charges with a temperature of 300 K.

In Fig. 7, we display how the activity changes within the EDL for 3 concentrations, for surface charges of  $\pm 0.2 \text{ C m}^{-2}$ . As expected from the previously described EDL profiles in Figs. 2-4, the activity of cations increases at negative electrodes, but decreases towards positive electrodes. This change is more pronounced with increasing concentration. Analogously, the anion activity decreases in the EDL of negative electrodes, but increases in positive EDLs, with larger effects for more concentration solutions. Whereas, we find the activity of water increases for both polarizations of the electrode, since water is attracted by electric fields.

While we can determine the activity of species in the EDL [101], which is commonly used terminology in the electrocatalysis community [102], we note that this can lead to some confusion. In the Nernst equation, the electrochemical equilibrium between the oxidised and reduced species is considered in the bulk [61, 65]. We also investigate the changes in composition in the EDL from establishing the equilibrium with the bulk, which is conceptually similar to the Nernst equilibrium. However, the Nernst equation considers the changes in chemical potential of the species with composition, while the EDL has a changing composition from the applied field, but the chemical potential of the species are equal to their bulk values [64, 73]. Therefore, one must not think that the activity of species within the EDL can drastically change the redox potentials. The relevant quantities within the EDL are

the concentrations of species, but these quantities sit in kinetic equations for these electron transfer processes, not for thermodynamic changes.

## V. DISCUSSION

Here, we presented a theory validated from MD simulations that predicts the structure of the EDL in 21m LiTFSI WiSE [73], in addition to the thermodynamic activity of the species [61], which allows for statements about changes in stability and reactivity towards interphase formation of the electrolyte. Our theory is simple, analytical and has at most one free fitting parameter ( $\alpha$ ), with the handful of parameters it does have being easily obtained from MD simulations [60]. Moreover, it directly links changes in coordination environments to these changes in activity, therefore, confirming correlations between data that have previously been drawn. We believe our approach has utility over others, such as the liquid-Madelung potential [59] or OPAS [61, 65], since only one MD simulation is required to parameterize the model, which can then make predictions over different compositions in the bulk and the EDL.

Not only that, but our approach can be extended to other electrolyte systems readily. For example, we have also studied ionic liquids [62], salt-in-ionic liquids [63, 72] and several conventional carbonate battery electrolytes [65, 75]. In terms of battery electrolytes, Phelan *et al.* [65] found similar trends in activity of salt and solvents. These predictions were validated from OPAS MD simulations, and also shifts in the  $\text{Li}^+/\text{Li}$  redox potential experimentally [65]. There, the liquid-Madelung potential was also compared [59], where much worse agreement with MD OPAS and experimental measurements was found [65].

Therefore, our formalism can be applied to a wide variety of electrolytes of interest in energy storage technologies. As described in the Theory Section, the presented version of the theory can only strictly be applied to an electrolyte where 2 components have  $f_i > 2$ , otherwise it is not known how the aggregates are connected [103]. However, despite this, the mass action laws, conservation of associations, and expressions for the free concentrations of ions are independent of this approximation, and can be applied more generally to more complicated electrolytes with more components [103]. These equations are

$$\Gamma_{ij}\lambda_{ij} = \frac{p_{ij}p_{ji}}{(1 - \sum_{j'} p_{ij'})(1 - \sum_{i'} p_{j'i'})}, \quad (44)$$

$$\Gamma_{ij} = \psi_i p_{ij} = \psi_j p_{ji}, \quad (45)$$

$$\phi_{f,i} = \phi_i \left( 1 - \sum_{j'} p_{ij'} \right)^{f_i}, \quad (46)$$

where  $\phi_{f,i}$  has been used to denote the free volume fraction of species  $i$ . While these equations allow for less restrictive functionalities to be used (any choice of functionality can be used), the electrolyte should still adhere to other assumptions of the theory (such as branched aggregates forming, instead of crystalline phases, and an association being well described by one association constant/environment [104]), and needs to be well described by these approximations.

Moreover, using these association probabilities, we can use them in the activity expressions

$$\ln(a_i) = \ln(\phi_{f,i}) = \ln \phi_i + f_i \ln \left( 1 - \sum_{j'} p_{ij'} \right). \quad (47)$$

Again note, that this form of the activity assumes the species only interact through associations. Using this, we can discuss more generally design principles of electrolytes to shift the activities in desired directions. To increase the activity of a species  $i$ , we can increase the concentration of  $i$  or reduce  $\sum_{j'} p_{ij'}$ . While we have direct control over the composition of the electrolyte, how the species interact and coordinate is determined more by their chemistry, but chemistries can be tuned in a way to reduce these association probabilities. For example, in the context of high entropy electrolytes for Li-metal anodes, it was suggested that more components of a similar chemistry improves transport properties, but keeps the stability of the electrolyte [105]. It is clear from Eq. (47) and the discussion in Ref. 75, that the salt activity of a high entropy electrolyte wouldn't be altered, which is consistent with experimentally observations [105]. With the generalised approach, we can also understand the many-anion high-entropy electrolytes [106]. Provided all anions interact with the cation with the same association constant, have the same functionality, and the overall volume fraction of anions is the same, there should then again be no net effect on activity. Any changes in these variables could, however, alter the predictions of activity, but it is likely their changes would be small (compared to the large changes over a wide range of salt concentrations). In those many anion high entropy electrolytes, similar SEI forming abilities

were reported, which we can corroborate with our approach. In addition, improved transport properties and operating temperatures were reported [106], but further developments are required to make design principles for transport properties.

Moreover, the EDL theory developed is built on the equilibrium of free species [64]. Therefore, a general closure relation can be stated

$$\bar{\phi}_{f,i} = \phi_{f,i} F(\Phi, \nabla\Phi, \alpha), \quad (48)$$

where  $F(\Phi, \nabla\Phi, \alpha)$  is the response of the species to electrostatic potentials and fields. Note that an equivalent set of mass action laws and conservation of associations applies in the EDL [64]. Therefore, the EDL can be investigated for more complicated electrolytes.

What this approach lacks, however, is the microscopic insight into changes in association constants with composition [63]. This could, however, be overcome empirically, and this simpler set of equations might provide more utility than the full complexity of the theory presented here.

In the context of interphase formation, we have several key thermodynamic insights, that can be widely applied to other electrolyte systems. However, the role of the electrode in our theory, and also simulation, is somewhat lacking, other than it holding the charge in the EDL. This was identified in Ref. 74, where specifically the Helmholtz layer solvation environments of conventional battery electrolytes was studied. However, that approach was still mainly focused on the electrolyte properties, with the role of the electrode entering through a reduction in the apparent functionality of species (and a generic surface interaction potential). Therefore, to get more insight into the role of different electrodes, such as Li-metal vs graphite, these surface interactions need to be included more explicitly.

Finally, while we have discussed thermodynamic effects from our simple model which provides insight into interphase formation, it still cannot directly predict what is going to form in the SEI or CEI. The changes in activity correlate with changes in frontier orbitals [65], but this does not provide an explicit link with interphase formation. Therefore, while our approach can provide guiding principles, to get chemically accurate predictions of interphase formation, atomistic approaches are necessary. Such approaches could be reaction networks, MLIPs, adiabatic energy surfaces from DFT for CIET. While computationally challenging, these approaches can provide the chemical insight lacking in our approach.

## VI. CONCLUSION

Overall, we extended our comparison between atomistic molecular dynamics simulations and theory of the EDL in LiTFSI WiSE to 21m. To achieve this from theory, we used the Boltzmann closure relations and introduce a charge rescaling factor. Qualitatively, good agreement with theory and simulation was found. This theory was then used to predict thermodynamic effect which could influence the stability and reactivity towards interphase formation. We first computed the changes in activity in the bulk, where we found these changes should result in a positive increase in the redox potentials for the formation of Li salts, such as LiF, in the SEI and thermodynamically suppress the hydrogen evolution reaction at negative potentials. The influence of the activity change on the oxygen evolution reaction are also explored. In addition, we used the equilibrium EDL concentrations to make predictions about how the kinetics of these reactions could be affected, where we found the formation of aggregates in the EDL should facilitate the formation of Li salts in the SEI. We presented a discussion of how this formalism could be extended to more complicated electrolytes, and applied to a wide variety of energy storage technologies.

## VII. ACKNOWLEDGMENTS

We are grateful to J. Pedro de Souza for the helpful discussions. D.M.M. & M.Z.B. acknowledge support from the Center for Enhanced Nanofluidic Transport 2 (CENT<sup>2</sup>), an Energy Frontier Research Center funded by the U.S. Department of Energy (DOE), Office of Science, Basic Energy Sciences (BES), under award # DE-SC0019112. D.M.M. also acknowledges support from the National Science Foundation Graduate Research Fellowship under Grant No. 2141064. M.M. and M.Z.B. acknowledge support from an Amar G. Bose Research Grant. Z.A.H.G acknowledges support through the Glasstone Research Fellowship in Materials and The Queen’s College, University of Oxford. Q.Z. & R.M.E.-M thanks the National Science for partially funding this research under National Science Foundation grants DMR 1904681 and CBET 1916609. This work was partially supported by the U.S. Army DEVCOM ARL Army Research Office (ARO) Energy Sciences Competency, Electrochemistry Program award # W911NF-24-1-0209. The views and conclusions contained in this document are those of the authors and should not be interpreted as representing the

official policies, either expressed or implied, of the U.S. Army or the U.S. Government.

---

- [1] K. Xu, Chem. Rev. **104**, 4303 (2004).
- [2] J. B. Goodenough and K. S. Park, “The Li-ion rechargeable battery: A perspective,” (2013).
- [3] K. Xu, Chem. Rev. **114**, 11503 (2014).
- [4] J. Zheng, J. A. Lochala, A. Kwok, Z. D. Deng, and J. Xiao, Adv. Sci. **4**, 1700032 (2017).
- [5] M. Li, C. Wang, Z. Chen, K. Xu, and J. Lu, Chem. Rev. (2020).
- [6] Y. Tian, G. Zeng, A. Rutt, T. Shi, H. Kim, J. Wang, J. Koettgen, Y. Sun, B. Ouyang, T. Chen, Z. Lun, Z. Rong, K. Persson, and G. Ceder, Chem. Rev. **121**, 1623 (2021).
- [7] K. Xu, Commun. Mater **3**, 31 (2022).
- [8] Z. Piao, R. Gao, Y. Liu, G. Zhou, and H.-M. Cheng, Adv.Mater. , 2206009 (2023).
- [9] H. Cheng, Q. Sun, L. Li, Y. Zou, Y. Wang, T. Cai, F. Zhao, G. Liu, Z. Ma, W. Wahyudi, Q. Li, and J. Ming, ACS Energy Lett. **7**, 490 (2022).
- [10] Y. Xie, J. Wang, B. H. Savitzky, Z. Chen, Y. Wang, S. Betzler, K. Bustillo, K. Persson, Y. Cui, L.-W. Wang, C. Ophus, P. Ercius, and H. Zheng, Sci. Adv. **9**, eadc9721 (2023).
- [11] S. Orangi, N. Manjong, D. P. Clos, L. Usai, O. S. Burheim, and A. H. Stromman, Journal of Energy Storage **76**, 109800 (2024).
- [12] H. Wang, Z. Yu, X. Kong, S. C. Kim, D. T. Boyle, J. Qin, Z. Bao, and Y. Cui, Joule **6**, 588 (2022).
- [13] Z. Yu, H. Wang, X. Kong, W. Huang, Y. Tsao, D. G. Mackanic, K. Wang, X. Wang, W. Huang, S. Choudhury, *et al.*, Nat. Energy **5**, 526 (2020).
- [14] Z. Yu, P. E. Rudnicki, Z. Zhang, Z. Huang, H. Celik, S. T. Oyakhire, Y. Chen, X. Kong, S. C. Kim, X. Xiao, *et al.*, Nat. Energy **7**, 94 (2022).
- [15] W. Li, E. M. Erickson, and A. Manthiram, Nat. Energy **5**, 26 (2020).
- [16] L. Qin, N. Xiao, J. Zheng, Y. Lei, D. Zhai, and Y. Wu, Adv. Energy Mater. **9**, 1902618 (2019).
- [17] J. Zheng, S. Chen, W. Zhao, J. Song, M. H. Engelhard, and J.-G. Zhang, ACS Energy Lett. **3**, 315 (2018).
- [18] S. Chen, Q. Nian, L. Zheng, B.-Q. Xiong, Z. Wang, Y. Shen, and X. Ren, J. Mater. Chem. A **9**, 22347 (2021).

- [19] F. Wang, O. Borodin, M. S. Ding, M. Gobet, J. Vatamanu, X. Fan, T. Gao, N. Edison, Y. Liang, W. Sun, *et al.*, *Joule* **2**, 927 (2018).
- [20] H. Zhang, B. Qin, J. Han, and S. Passerini, *ACS Energy Lett.* **3**, 1769 (2018).
- [21] Q. Dou, S. Lei, D.-W. Wang, Q. Zhang, D. Xiao, H. Guo, A. Wang, H. Yang, Y. Li, S. Shi, and X. Yan, *Energy Environ. Sci.* **11**, 3212 (2018).
- [22] Q. Dou, Y. Lu, L. Su, X. Zhang, S. Lei, X. Bu, L. Liu, D. Xiao, J. Chen, S. Shi, and X. Yan, *Energy Storage Materials* **23** (2019), 10.1016/j.ensm.2019.03.016.
- [23] N. Molinari and B. Kozinsky, *J. Phys. Chem. B* **124**, 2676 (2020).
- [24] M. Y. Lui, L. Crowhurst, J. P. Hallett, P. A. Hunt, H. Niedermeyer, and T. Welton, *Chem. Sci.* **2**, 1491 (2011).
- [25] L. Suo, O. Borodin, W. Sun, X. Fan, C. Yang, F. Wang, T. Gao, Z. Ma, M. Schroeder, A. von Cresce, S. M. Russell, M. Armand, A. Angell, K. Xu, and C. Wang, *Angew. Chem.* **55**, 7136 (2016).
- [26] S. Kondou, E. Nozaki, S. Terada, M. L. Thomas, K. Ueno, Y. Umebayashi, K. Dokko, and M. Watanabe, *The Journal of Physical Chemistry C* **122**, 20167 (2018).
- [27] N. Molinari, J. P. Mailoa, N. Craig, J. Christensen, and B. Kozinsky, *J. Power Sources* **428**, 27 (2019).
- [28] N. Molinari, J. P. Mailoa, and B. Kozinsky, *J. Phys. Chem. Lett.* **10**, 2313 (2019).
- [29] L. Chen, J. Zhang, Q. Li, J. Vatamanu, X. Ji, T. P. Pollard, C. Cui, S. Hou, J. Chen, C. Yang, *et al.*, *ACS Energy Lett.* (2020).
- [30] L. Jiang, L. Liu, J. Yue, Q. Zhang, A. Zhou, O. Borodin, L. Suo, H. Li, L. Chen, K. Xu, and Y. Hu, *ADV MATER* **32**, 1904427 (2020).
- [31] M. Becker, D. Reber, A. Aribia, C. Battaglia, and R.-S. Kühnel, (2020).
- [32] I.-B. Magdău, D. J. Arismendi-Arrieta, H. E. Smith, C. P. Grey, K. Hermansson, and G. Csányi, *npj Computational Materials* volume **9**, 146 (2023).
- [33] N. Yao, X. Chen, Z.-H. Fu, and Q. Zhang, *Chem. Rev.* **122**, 10970 (2022).
- [34] Z. A. Goodwin, M. B. Wenny, J. H. Yang, A. Cepellotti, J. Ding, K. Bystrom, B. R. Duschatko, A. Johansson, L. Sun, S. Bätzner, A. Musaelian, J. A. Mason, B. Kozinsky, and N. Molinari, *J. Phys. Chem. Lett.* **15**, 7539 (2024).
- [35] J. H. Yang, A. W. S. Ooi, Z. A. Goodwin, Y. Xie, J. Ding, S. Falletta, A.-H. A. Park, and B. Kozinsky, *J. Phys. Chem. Lett.* **16**, 3039 (2025).

- [36] H. Zhang, V. Juraskova, and F. Duarte, *Nat. Commun* **15**, 6114 (2024).
- [37] V. Juraskova, G. Tusha, H. Zhang, L. V. Schäfer, and F. Duarte, *Faraday Discussion* **256**, 156 (2025).
- [38] K. Xu, Y. Lam, S. S. Zhang, T. R. Jow, and T. B. Curtis, *The Journal of Physical Chemistry C* **111**, 7411 (2007).
- [39] A. von Wald Cresce, O. Borodin, and K. Xu, *The Journal of Physical Chemistry C* **116**, 26111 (2012).
- [40] O. Borodin, J. Self, K. A. Persson, C. Wang, and K. Xu, *Joule* **4**, 69 (2020).
- [41] R. Andersson, F. Årén, A. A. Franco, and P. Johansson, *Journal of the Electrochemical Society* **167**, 140537 (2020).
- [42] H. Wang, S. C. Kim, T. Rojas, Y. Zhu, Y. Li, L. Ma, K. Xu, A. T. Ngo, and Y. Cui, *J. Am. Chem. Soc.* **143**, 2264 (2021).
- [43] S. C. Kim, X. Kong, R. A. Vilá, W. Huang, Y. Chen, D. T. Boyle, Z. Yu, H. Wang, Z. Bao, J. Qin, and Y. Cui, *J. Am. Chem. Soc.* **143**, 10301 (2021).
- [44] O. O. Postupna, Y. V. Kolesnik, O. N. Kalugin, and O. V. Prezhdo, *J. Phys. Chem. B* **115**, 14563 (2011).
- [45] O. Borodin and D. Bedrov, *J. Phys. Chem. C* **118**, 18362 (2014).
- [46] Z. Li, O. Borodin, G. D. Smith, and D. Bedrov, *J. Phys. Chem. B* **119**, 3085 (2015).
- [47] I. Skarmoutsos, V. Ponnuchamy, V. Vetere, and S. Mossa, *J. Phys. Chem. C* **119**, 4502 (2015).
- [48] O. Borodin, X. Ren, J. Vatamanu, A. von Wald Cresce, J. Knap, and K. Xu, *Acc. Chem. Res.* **50**, 2886 (2017).
- [49] S. Han, *Sci. Rep.* **7**, 46718 (2017).
- [50] B. Ravikumar, M. Mynam, and B. Rai, *J. Phys. Chem. C* **122**, 8173 (2018).
- [51] Y. Shim, *Phys. Chem. Chem. Phys.* **20**, 28649 (2018).
- [52] S. Han, *Sci. Rep.* **9**, 5555 (2019).
- [53] N. Piao, X. Ji, H. Xu, X. Fan, L. Chen, S. Liu, M. N. Garaga, S. G. Greenbaum, L. Wang, C. Wang, and X. He, *Adv. Energy Mater.* **10**, 1903568 (2020).
- [54] T. Hou, K. D. Fong, J. Wang, and K. A. Persson, *Chem. Sci.* **12**, 14740 (2021).
- [55] Y. Wu, A. Wang, Q. Hu, H. Liang, H. Xu, L. Wang, and X. He, *ACS Cent. Sci.* **8**, 1290 (2022).

- [56] A. V. Cresce, S. M. Russell, O. Borodin, J. A. Allen, M. A. Schroeder, M. Dai, J. Peng, M. P. Gobet, S. G. Greenbaum, R. E. Rogers, and K. Xu, *Phys. Chem. Chem. Phys.* **19**, 574 (2017).
- [57] S. P. Beltran, X. Cao, J.-G. Zhang, and P. B. Balbuena, *Chem. Mater.* **32**, 5973 (2020).
- [58] Q. Wu, M. T. McDowell, and Y. Qi, *JACS* **145**, 2473 (2023).
- [59] N. Takenaka, S. Ko, A. Kitada, and A. Yamada, *Nature Communications* **15**, 1319 (2024).
- [60] M. McEldrew, Z. A. Goodwin, S. Bi, M. Z. Bazant, and A. A. Kornyshev, *J. Chem. Phys.* **152**, 234506 (2020).
- [61] M. McEldrew, Z. A. Goodwin, S. Bi, A. Kornyshev, and M. Z. Bazant, *J. Electrochem. Soc.* **168**, 050514 (2021).
- [62] M. McEldrew, Z. A. H. Goodwin, H. Zhao, M. Z. Bazant, and A. A. Kornyshev, *J. Phys. Chem B* **125**, 2677–2689 (2021).
- [63] M. McEldrew, Z. A. H. Goodwin, N. Molinari, B. Kozinsky, A. A. Kornyshev, and M. Z. Bazant, *J. Phys. Chem. B* **125**, 13752 (2021).
- [64] Z. A. Goodwin, M. McEldrew, J. P. de Souza, M. Z. Bazant, and A. A. Kornyshev, *J. Chem. Phys.* **157**, 094106 (2022).
- [65] C. Phelan, A. Bhandari, J. Singh, M. F. nad Erik Björklund, J. Swallow, P. Bencok, C. Grey, Z. Goodwin, C. Skylaris, and R. Weatherup, <https://chemrxiv.org/doi/pdf/10.26434/chemrxiv-2025-k903g> (2025).
- [66] A. A. Kornyshev, *J. Phys. Chem. B* **111**, 5545 (2007).
- [67] M. S. Kilic, M. Z. Bazant, and A. Ajdari, *Physical review E* **75**, 021502 (2007).
- [68] Z. A. H. Goodwin, G. Feng, and A. A. Kornyshev, *Electrochim. Acta* **225**, 190 (2017).
- [69] M. Z. Bazant, M. S. Kilic, B. D. Storey, and A. Ajdari, *Advances in colloid and interface science* **152**, 48 (2009).
- [70] J. P. de Souza, Z. A. Goodwin, M. McEldrew, A. A. Kornyshev, and M. Z. Bazant, *Phys. Rev. Lett.* **125**, 116001 (2020).
- [71] Z. A. Goodwin and A. A. Kornyshev, *Electrochim. Acta* **434**, 141163 (2022).
- [72] D. M. Markiewitz, Z. A. Goodwin, M. McEldrew, J. P. de Souza, X. Zhang, R. M. Espinosa-Marzal, and M. Z. Bazant, *Faraday Discussions*, 365 (2024).
- [73] D. M. Markiewitz, Z. A. Goodwin, Q. Zheng, M. McEldrew, R. M. Espinosa-Marzal, and M. Z. Bazant, *ACS Applied Materials & Interfaces* **17**, 29515 (2025).

- [74] Z. A. Goodwin, D. M. Markiewitz, Q. Wu, Y. Qi, and M. Z. Bazant, *ACS Applied Energy Materials* **8**, 8376 (2025).
- [75] Z. A. H. Goodwin, M. McEldrew, B. Kozinsky, and M. Z. Bazant, *PRX Energy* **2**, 013007 (2023).
- [76] L. Suo, Y.-S. Hu, H. Li, M. Armand, and L. Chen, *Nat. Commun.* **4**, 1481 (2013).
- [77] L. Suo, O. Borodin, T. Gao, M. Olguin, J. Ho, X. Fan, C. Luo, C. Wang, and K. Xu, *Science* **350**, 938 (2015).
- [78] J. Wang, Y. Yamada, K. Sodeyama, C. H. Chiang, Y. Tateyama, and A. Yamada, *Nat. Commun.* **7**, 12032 (2016).
- [79] F. Wang, O. Borodin, T. Gao, X. Fan, W. Sun, F. Han, A. Faraone, J. A. Dura, K. Xu, and C. Wang, *Nature Materials* **17**, 543 (2018).
- [80] Y. Yamada, K. Usui, K. Sodeyama, S. Ko, Y. Tateyama, and A. Yamada, *Nat. Energy* **1**, 16129 (2016).
- [81] L. Suo, O. Borodin, Y. Wang, X. Rong, W. Sun, X. Fan, S. Xu, M. A. Schroeder, A. V. Cresce, F. Wang, *et al.*, *Advanced Energy Materials* **7**, 1701189 (2017).
- [82] J. Vatamanu and O. Borodin, *J. Phys. Chem. Lett.* **8**, 4362 (2017).
- [83] M. McEldrew, Z. A. Goodwin, A. A. Kornyshev, and M. Z. Bazant, *The journal of physical chemistry letters* **9**, 5840 (2018).
- [84] S. Sayah, A. Ghosh, M. Baazizi, R. Amine, M. Dahbi, Y. Amine, F. Ghamouss, and K. Amine, *Nano Energy* **98**, 107336 (2022).
- [85] O. Borodin, L. Suo, M. Gobet, X. Ren, F. Wang, A. Faraone, J. Peng, M. Olguin, M. Schroeder, M. S. Ding, *et al.*, *ACS nano* **11**, 10462 (2017).
- [86] J. Zheng, G. Tan, P. Shan, T. Liu, J. Hu, Y. Feng, L. Yang, M. Zhang, Z. Chen, Y. Lin, *et al.*, *Chem* **4**, 2872 (2018).
- [87] J. Lim, K. Park, H. Lee, J. Kim, K. Kwak, and M. Cho, *Journal of the American Chemical Society* **140**, 15661 (2018).
- [88] Z. Yu, L. A. Curtiss, R. E. Winans, Y. Zhang, T. Li, and L. Cheng, *The Journal of Physical Chemistry Letters* **11**, 1276 (2020).
- [89] R. Zhang, M. Han, K. Ta, K. E. Madsen, X. Chen, X. Zhang, R. M. Espinosa-Marzal, and A. A. Gewirth, *ACS Applied Energy Materials* **3**, 8086 (2020).
- [90] M. Han, R. Zhang, A. A. Gewirth, and R. M. Espinosa-Marzal, *Nano Lett.* **21**, 2304 (2021).

- [91] T. Ichii, S. Ichikawa, Y. Yamada, M. Murata, T. Utsunomiya, and H. Sugimura, *Japanese Journal of Applied Physics* **59**, SN1003 (2020).
- [92] C.-Y. Li, M. Chen, S. Liu, X. Lu, J. Meng, J. Yan, H. D. Abruña, G. Feng, and T. Lian, *Nature Communications* **13**, 5330 (2022).
- [93] X. Zhang, Z. A. Goodwin, A. G. Hoane, A. Deptula, D. M. Markiewitz, N. Molinari, Q. Zheng, H. Li, M. McEldrew, B. Kozinsky, *et al.*, *ACS nano* **18**, 34007 (2024).
- [94] A. Daggetti, S. Romeo, M. Uselli, and S. Trasatti, *J. CHEM. SOC. FARADAY TRANS.* **89**, 187 (1993).
- [95] H.-G. Steinrück, C. Cao, M. R. Lukatskaya, C. J. Takacs, G. Wan, D. G. Mackanic, Y. Tsao, J. Zhao, B. A. Helms, K. Xu, *et al.*, *Angew. Chem.* (2020).
- [96] C. M. Phelan, E. Björklund, J. Singh, M. Fraser, P. N. Didwal, G. J. Rees, Z. Ruff, P. Ferrer, D. C. Grinter, C. P. Grey, *et al.*, *Chemistry of Materials* **36**, 3334 (2024).
- [97] E. Bjorklund, C. Xu, W. M. Dose, C. G. Sole, P. K. Thakur, T.-L. Lee, M. F. De Volder, C. P. Grey, and R. S. Weatherup, *Chemistry of Materials* **34**, 2034 (2022).
- [98] B. L. Rinkel, D. S. Hall, I. Temprano, and C. P. Grey, *Journal of the American Chemical Society* **142**, 15058 (2020).
- [99] B. L. Rinkel, J. P. Vivek, N. Garcia-Araez, and C. P. Grey, *Energy & environmental science* **15**, 3416 (2022).
- [100] M. V. Fedorov and A. A. Kornyshev, *Chem. Rev.* **114**, 2978 (2014).
- [101] A. R. Finney, I. J. McPherson, P. R. Unwin, and M. Salvalaglio, *Chemical Science* **12**, 11166 (2021).
- [102] M. A. Gebbie, B. Liu, W. Guo, S. R. Anderson, and S. G. Johnstone, *ACS Catal.* **13**, 16222 (2023).
- [103] M. McEldrew, *Ion Aggregation, Correlated Ion Transport and the Double Layer in Super-Concentrated Electrolytes*, Ph.D. thesis, MIT (2021).
- [104] A. V. Tkachenko, C. Cao, A. C. Marschilok, and D. Lu, arXiv:2512.18167 (2025).
- [105] S. C. Kim, J. Wang, R. Xu, P. Zhang, Y. Chen, Z. Huang, Y. Yang, Z. Yu, S. T. Oyakhire, W. Zhang, L. C. Greenburg, M. S. Kim, D. T. Boyle, P. Sayavong, Y. Ye, J. Qin, Z. Bao, and Y. Cui, *Nature Energy* **8**, 814 ((2023)).
- [106] Q. Wang, C. Zhao, J. Wang, Z. Yao, S. Wang, S. G. H. Kumar, S. Ganapathy, S. Eustace, X. Bai, B. Li, and M. Wagemaker, *Nat. Commun.* **14**, 440 (2023).